[CANCER RESEARCH 63, 6447–6452, October 1, 2003]

The Breast Cancer Resistance Protein (Bcrp1/Abcg2) Restricts Exposure to the Dietary Carcinogen 2-Amino-1-methyl-6-phenylimidazo[4,5-b]pyridine[1]

Antonius E. van Herwaarden, Johan W. Jonker, Els Wagenaar, Remco F. Brinkhuis, Jan H. M. Schellens, Jos H. Beijnen, and Alfred H. Schinkel[2]

Division of Experimental Therapy [A. E. v. H., J. W. J., E. W., R. F. B., A. H. S.] and Divisions of Experimental Therapy and Medical Oncology [J. H. M. S.], The Netherlands Cancer Institute, 1066 CX Amsterdam, and Department of Pharmacy and Pharmacology, Slotervaart Hospital, 1066 EC Amsterdam [J. H. B.], The Netherlands

ABSTRACT

The food carcinogen 2-amino-1-methyl-6-phenylimidazo[4,5-b]pyridine (PhIP) is the most abundant heterocyclic amine found in various protein containing foods. PhIP is mutagenic and carcinogenic in rodents, inducing lymphomas in mice and colon, mammary and prostate carcinomas in rats. It has also been implicated in human breast carcinogenesis. Humans on a normal Western diet are exposed to PhIP on a daily basis. The breast cancer resistance protein (BCRP/ABCG2) transports various anticancer drugs from cells, causing multidrug resistance. By its presence in the apical membrane of the intestine and bile canalicular membrane, it also protects the body from substrate drugs and toxins. We investigated whether Bcrp1 could affect PhIP exposure of the body because this could implicate BCRP activity in the cancer risk due to PhIP. Using polarized cell lines, we found that PhIP is efficiently transported by murine Bcrp1. *In vivo* pharmacokinetic studies showed that at a dose of 1 mg/kg [^{14}C]PhIP the area under the curve for oral administration was 2.9-fold higher in *Bcrp1*$^{-/-}$ compared with wild-type mice (306 ± 39 *versus* 107 ± 15 h·ng/ml) and, for i.v. administration, 2.2 fold higher (386 ± 36 *versus* 178 ± 8.9 h·ng/ml). Wild-type mice cleared [^{14}C]PhIP mainly by fecal excretion, but this shifted to primarily urinary excretion in *Bcrp1*$^{-/-}$ mice. In mice with a cannulated gall bladder, both hepatobiliary and direct intestinal excretion of [^{14}C]PhIP were greatly impaired in *Bcrp1*$^{-/-}$ compared with wild-type mice (9.0 ± 4.4 *versus* 36.5 ± 9.4% and 1.5 ± 0.8 *versus* 4.2 ± 1.5%, respectively). We conclude that Bcrp1 effectively restricts the exposure of mice to ingested PhIP by decreasing its uptake from the gut lumen and by mediating hepatobiliary and intestinal elimination. Intra- or interindividual differences in BCRP activity in humans may thus also affect the exposure to PhIP and related food carcinogens, with possible implications for cancer susceptibility.

INTRODUCTION

Epidemiological studies have associated the consumption of well-done meat, containing high levels of HAs, with an increased risk of intestinal and breast cancer (1). The HAs are a family of mutagenic and carcinogenic compounds formed by pyrolysis reactions during the cooking of protein-containing foods such as meat and fish (2–4). HAs can be detected in the urine of healthy volunteers on a normal diet, and exposure occurs on a daily basis (5, 6). Among the five principal HAs, PhIP is the most abundant in the diet, present in cooked meat and fish at levels of 0.56–69.2 ng/g and in cigarette smoke condensate (2, 5, 7, 8). PhIP is a very potent mutagen in the Ames/*Salmonella* assay (2). The administration of PhIP to F344 rats leads to aberrant crypt foci and adenocarcinomas in the colon (3). The carcinogenic potential of PhIP in the colon appears to be strain dependent, indicating that interactions between the environmental exposure (PhIP) and genetic make-up are important in this process (9). PhIP induces lymphomas in mice and mammary and prostate carcinomas in rats as well (3, 10–13). PhIP may also be a mammary carcinogen in humans (14). The incremental cancer risk attributable to dietary intake of HAs in humans in the developed world has been estimated to be 1.1×10^{-4}, wherein PhIP contributes up to 46% of this incremental risk (7).

BCRP is a member of the ABC family of drug transporters. It can actively transport various anticancer drugs (doxorubicin, mitoxantrone, and topotecan) from cells, causing multidrug resistance (15, 16). The mouse homologue Bcrp1 is present in the apical membrane of epithelial cells of the small intestine, colon, cecum, and renal proximal tubules, in hepatic bile canalicular membranes, and in placental labyrinth cells (17, 18). We previously demonstrated that this enables Bcrp1 to decrease the oral uptake and fetal penetration of topotecan and dietary compounds (17, 18). Because BCRP/Bcrp1 plays a role in the (re-)uptake from the gut, the hepatobiliary excretion and the overall clearance of topotecan and presumably other BCRP substrates, we were interested in the possible role of Bcrp1 in the bioavailability of dietary carcinogens such as PhIP.

If BCRP would have a role in protection from food carcinogens, then inter- or intraindividual variation in BCRP activity, as a consequence of induction, stimulation, or inhibition of BCRP by food or drug intake or because of BCRP polymorphisms, could be important to individual cancer susceptibility (19, 20). Dietrich *et al.* (21, 22) established that the ABC transporter MRP2 transports PhIP and affects its oral uptake and excretion using Mrp2 mutant rats. There might be analogous roles for BCRP and the ABC transporter P-gp because all three transporters are present in the apical membranes of small intestine and bile canalicular membrane. Each could thus potentially influence the bioavailability of xenotoxins and carcinogens. In this study, we addressed the question whether Bcrp1 and P-gp can transport PhIP and can affect its bioavailability by *in vitro* and *in vivo* studies using Bcrp1- and P-gp-knockout mice.

MATERIALS AND METHODS

Animals. Mice were housed and handled according to institutional guidelines complying with Dutch legislation. Animals used in all experiments were male *Bcrp1*$^{-/-}$, *Mdr1a/1b*$^{-/-}$, and wild-type mice, all of >99% FVB genetic background between 9 and 14 weeks of age. Animals were kept in a temperature-controlled environment with a 12-h light/12-h dark cycle. They received a standard diet (a.m.-II, Hope Farms, Woerden, The Netherlands) and acidified water *ad libitum*.

Chemicals. PhIP and [^{14}C]PhIP (10 mCi/mmol) were from Toronto Research Chemicals, Inc. (Toronto, Ontario, Canada); [^{3}H]]Inulin was from Amersham Pharmacia Biotech (Little Chalfont, Buckinghamshire, United Kingdom); ketamine (Ketanest-S) was from Parke-Davis (Hoofddorp, the Netherlands); xylazine was from Sigma Chemical Co. (St. Louis, MO); methoxyflurane (Metofane) was from Medical Developments Australia Pty. Ltd. (Springvale, Victoria, Australia); GF120918 was from GlaxoSmithKline (Research Triangle Park, North Carolina, USA); Ko143 was described previously (23).

Cells and Tissue Culture. The polarized pig kidney epithelial cell line LLC-PK1 and the polarized canine kidney cell line MDCK-II were used in the

Received 4/10/03; revised 6/25/03; accepted 7/9/03.

The costs of publication of this article were defrayed in part by the payment of page charges. This article must therefore be hereby marked *advertisement* in accordance with 18 U.S.C. Section 1734 solely to indicate this fact.

[1] This project was, in part, financially supported by the Dutch Cancer Society Grant NKI 2000-2271.

[2] To whom requests for reprints should be addressed, at Division of Experimental Therapy, The Netherlands Cancer Institute, Plesmanlaan 121, 1066 CX Amsterdam, the Netherlands. E-mail: a.schinkel@nki.nl.

[3] The abbreviations used are: HA, heterocyclic amine; PhIP, 2-amino-1-methyl-6-phenylimidazo[4,5-b]pyridine; ABC, ATP-binding cassette; BCRP, breast cancer resistance protein; P-gp, P-glycoprotein; AUC, area under the plasma concentration-time curve.

transport assays. Human *MDR1*-, and murine *Mdr1a*-, *Mdr1b*-, and *Bcrp1*-transfected LLC-PK1 subclones were described previously (17, 24, 25). The LLC-PK1 cells and transfected subclones were cultured in M199 medium supplied with L-glutamine (Life Technologies, Inc., Breda, the Netherlands) and supplemented with penicillin (50 units/ml), streptomycin (50 μg/ml) and 10% (v/v) FCS (Life Technologies, Inc.) at 37°C in the presence of 5% CO_2. Human *MDR1*-, murine *Bcrp1*-, and human *MRP2*-transduced MDCK-II subclones were described previously (17, 26). The MDCK-II cells and transduced subclones were cultured in DMEM supplied with glutamax (Life Technologies, Inc.) and supplemented with penicillin (50 units/ml), streptomycin (50 μg/ml), and 10% (v/v) FCS (Life Technologies, Inc.) at 37°C in the presence of 5% CO_2.

Transport Assay. Transport assays were carried out as described with minor modifications (24). Cells were seeded on microporous polycarbonate membrane filters (3.0-μm pore size, 24 mm diameter, Transwell 3414; Costar, Corning, NY) at a density of 2.0×10^6 cells/well in 2 ml of complete medium. Cells were grown for 3 days, and medium was replaced every day. Two h before the start of the experiment, medium at both the apical and basolateral side of the monolayer was replaced with 2 ml of Optimem medium (Life Technologies, Inc.) without serum, either with or without 5 μM GF120918 or Ko143. The experiment was started (t = 0) by replacing the medium in either the apical or basolateral compartment with fresh Optimem medium, either with or without 5 μM GF120918 or Ko143 and 2 or 100 μM [^{14}C]PhIP and [^{3}H]]inulin. Cells were incubated at 37°C in 5% CO_2, and 50 μl of aliquots were taken every hour. The appearance of radioactivity in the opposite compartment was measured and presented as the fraction of total radioactivity added at the beginning of the experiment. The tightness of the monolayer was measured by monitoring the paracellular flux of [^{3}H]]inulin to the opposite compartment, which had to remain <1.5% of the total radioactivity/hour.

Pharmacokinetic Experiments. For i.v. administration of [^{14}C]PhIP, 5 μl of drug solution [appropriate concentration in 20% (v/v) DMSO, 4% (w/v) D-glucose]/g body weight was injected into the tail vein of mice lightly anesthetized with methoxyflurane. For oral administration, 5.3 μl of drug solution [appropriate concentration in 5.8% (v/v) DMSO, 4.7% (w/v) D-glucose, 0.01 M HCl]/g body weight were dosed by gavage into the stomach. Animals were sacrificed by terminal bleeding through cardiac puncture after anesthesia with methoxyflurane. Levels of radioactivity in plasma and urine were determined by liquid scintillation counting.

Metabolic Cage Experiment. Mice were housed in a Ruco Type M/1 metabolic cage (Valkenswaard, the Netherlands). They were allowed to accustom to the cages for 2 days, before receiving [^{14}C]PhIP (1 mg/kg) injected into the tail vein under light anesthesia with methoxyflurane. Feces and urine were collected in fractions of 0–4, 4–8, 8–24, and 24–48 h after drug administration, and feces was homogenized in 4% (w/v) BSA. Levels of radioactivity in feces and urine were determined by liquid scintillation counting.

Gall Bladder Cannulation Experiments. Mice were anesthetized with a combination of ketamine (25 mg/ml) and xylazine to a final dose of 116 mg/kg ketamine and 8 mg/kg xylazine. The volume of the anesthetic solution injected i.p. was 5 μl/g body weight. After opening of the abdominal cavity and distal ligation of the common bile duct, a polythene catheter (Portex Limited, Hythe, United Kingdom), with an inner diameter of 0.28 mm, was inserted into the incised gall bladder. The catheter was fixed to the gall bladder with an additional ligation. Bile was collected in 10-min fractions for 60 min after i.v. injection of [^{14}C]PhIP (1 mg/kg) into the tail vein. At the end of the experiment, blood was collected by cardiac puncture, and organs were removed and homogenized in 4% (w/v) BSA. Intestinal contents (feces) were separated from intestinal tissue. Levels of radioactivity in plasma, bile, feces, and tissue homogenates were determined by liquid scintillation counting.

Pharmacokinetic Calculations and Statistical Analysis. All values are given as average ± SD, unless indicated otherwise. A two-sample equal variance (homoscedastic) Student's *t* test was used to assess the significance of difference between two sets of data. Differences were considered to be statistically significant when $P < 0.05$. AUC from time = 0 to the last sampling point was calculated by the linear trapezoidal rule, and oral availability was determined by AUC p.o./AUC i.v. at a dose of 1 mg/kg.

RESULTS

***In Vitro* Transport of [^{14}C]PhIP by MDR1, Mdr1a, and Mdr1b P-gp and by MRP2 and Bcrp1.** To test whether Bcrp1 and P-gp are involved in PhIP transport *in vitro*, we made use of the polarized pig kidney epithelial cell line LLC-PK1 and its subclones transfected with human *MDR1*, murine *Mdr1a*, murine *Mdr1b*, or wild-type murine *Bcrp1* cDNAs, and the polarized canine kidney cell line MDCK-II and its subclones transduced with human *MDR1*, human *MRP2*, or murine *Bcrp1* cDNAs. The cell lines were grown to confluent polarized monolayers on porous membrane filters, and vectorial transport of [^{14}C]PhIP across the monolayer was determined. In the MDCK-II parental cell line, apically and basolaterally directed translocation of [^{14}C]PhIP (2 μM) were similar, and this was also the case for the *MRP2*-transduced MDCK-II subclone (Fig. 1, *A* and *B*). In the *MDR1*-transduced MDCK-II cells, there was somewhat increased apical and decreased basolateral translocation, whereas in the *Bcrp1*-transduced MDCK-II cell line, apically directed translocation was highly increased and basolaterally directed translocation drastically decreased (Fig. 1, *C* and *D*).

Subsequently, we tested [^{14}C]PhIP translocation by Mdr1a, Mdr1b, and MDR1 in the LLC-PK1 cell line. At a concentration of 2 μM [^{14}C]PhIP, there was a high background of apically directed translocation in the LLC-PK1 parent (see below), which was considerably reduced by increasing the [^{14}C]PhIP concentration to 100 μM. At this high concentration, [^{14}C]PhIP translocation in the LLC-PK1- *Mdr1b* and LLC-PK1-*MDR1* subclones was not different compared with the parental cell line (data not shown). However, for the *Mdr1a*-transfected LLC-PK1 subclone an increased apical and decreased basolateral translocation was observed (Fig. 2, *A* and *B*). In the *Bcrp1*-transfected LLC-PK1 subclone, apically directed translocation was highly increased and basolaterally directed translocation was highly decreased compared with the parental LLC-PK1 parent cell line (Fig. 2*C*). This transport was completely inhibited by Ko143, a selective Bcrp1 inhibitor (Fig. 2*D*; Ref. 23) and partially by the Bcrp1/P-gp inhibitor GF120918 (Fig. 2*E*; Ref. 27). This suggests that Ko143 is a better inhibitor of Bcrp1 than GF120918, consistent with Allen *et al.*

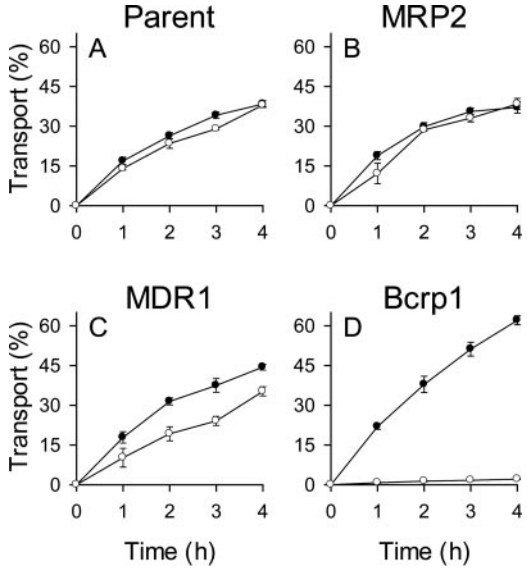

Fig. 1. Transepithelial transport of [^{14}C]PhIP (2 μM) in MDCK-II cells either non-transduced (*A*) or transduced with human *MRP2* (*B*), human *MDR1* (*C*), or murine *Bcrp1* (*D*) cDNAs. At t = 0, [^{14}C]PhIP was applied in one compartment (basolateral or apical), and the percentage of radioactivity appearing in the opposite compartment at t = 1, 2, 3, and 4 h was measured and plotted ($n = 3$). Translocation from the basolateral to the apical compartment (●); translocation from the apical to the basolateral compartment (○). *Error bars* (often smaller than the symbols) indicate SD.

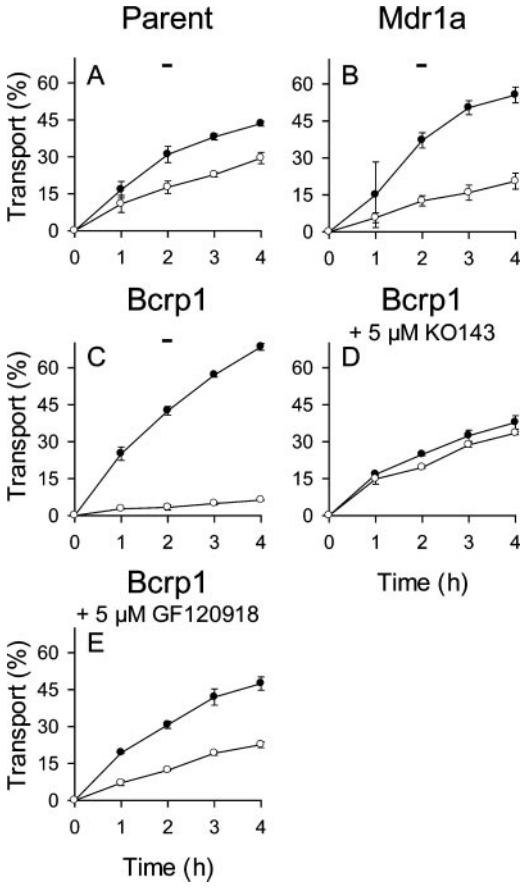

Fig. 2. Transepithelial transport of [^{14}C]PhIP (100 μM) in LLC-PK1 cells either nontransfected (*A*) or transfected with murine *Mdr1a* (*B*) or murine *Bcrp1* cDNA in the absence (*C*) or presence of Ko143 (*D*) or GF120918 (*E*). At t = 0, [^{14}C]PhIP was applied in one compartment (basolateral or apical), and the percentage of radioactivity appearing in the opposite compartment at t = 1, 2, 3, and 4 h was measured and plotted (n = 3). Translocation from the basolateral to the apical compartment (●); translocation from the apical to the basolateral compartment (○). *Error bars* (often smaller than the symbols) indicate SD.

(23), and that PhIP transport by Bcrp1 is not easily completely inhibited. The high background transport of [^{14}C]PhIP in parental LLC-PK1 cells (especially observed at 2 μM [^{14}C]PhIP) was most likely attributable to endogenous pig BCRP because this endogenous transport was nearly completely inhibited by both GF120918 and Ko143 (data not shown).

Taken together, the results demonstrate highly efficient transport of PhIP by Bcrp1, moderate transport by murine Mdr1a, and low transport by human MDR1.

***In Vivo* Plasma Pharmacokinetics of [^{14}C]PhIP in Bcrp1$^{-/-}$, Mdr1a/b$^{-/-}$, and Wild-Type Mice.** To assess whether the *in vitro* observed Bcrp1- and Mdr1a- mediated PhIP transport is also relevant *in vivo*, we tested the oral uptake of [^{14}C]PhIP in wild-type, *Mdr1a/b*$^{-/-}$, and *Bcrp1*$^{-/-}$ mice. One h after oral [^{14}C]PhIP administration at 1 mg/kg, [^{14}C]PhIP plasma levels of the *Bcrp1*$^{-/-}$ mice were increased 3.1-fold compared with the wild-type mice (144 ± 22 *versus* 46.3 ± 4.3 ng/ml, $P < 0.002$). In contrast, [^{14}C]PhIP plasma levels in the Mdr1a/b$^{-/-}$ mice did not differ from those in the wild-type mice (46.0 ± 18 *versus* 46.3 ± 4.3 ng/ml, $P = 0.98$).

The clear impact of the Bcrp1 genotype on oral [^{14}C]PhIP uptake incited a more extensive analysis of the underlying processes. We administered [^{14}C]PhIP (1 mg/kg) either p.o. or i.v. to *Bcrp1*$^{-/-}$ and wild-type mice. We observed that 15 min after oral administration, the plasma [^{14}C]PhIP level had already reached its maximum, suggesting rapid absorption from the intestines and rapid distribution and clearance (Fig. 3*A*). Plasma [^{14}C]PhIP levels also decreased quickly after i.v. administration (Fig. 3*B*), indicating a high distribution rate of PhIP and possibly a high clearance rate by liver and/or kidneys (see below). Within 7.5 min after i.v. administration, [^{14}C]PhIP plasma levels were lower in wild-type than in *Bcrp1*$^{-/-}$ mice, indicating that clearance/distribution differences arose early (Fig. 3*B*). Semilog plotting of the data showed that between 15 and 120 min after i.v. administration, the elimination rate constant was comparable between *Bcrp1*$^{-/-}$ and wild-type mice (data not shown).

At a dose of 1 mg/kg [^{14}C]PhIP, the AUC for oral administration was 2.9-fold higher in *Bcrp1*$^{-/-}$ compared with wild-type mice (306 ± 39 *versus* 107 ± 15 h·ng/ml). The AUC for i.v. administered [^{14}C]PhIP was 2.2-fold higher in *Bcrp1*$^{-/-}$ compared with wild-type mice (386 ± 36 *versus* 178 ± 8.9 h·ng/ml). The calculated oral availability was 79 ± 6 and 60 ± 5% for *Bcrp1*$^{-/-}$ and wild-type mice respectively, *i.e.,* moderately but significantly ($P < 0.01$) increased in *Bcrp1*$^{-/-}$ mice.

Fecal and Urinary Excretion of [^{14}C]PhIP in *Bcrp1*$^{-/-}$ and Wild-Type Mice. To determine the extent to which fecal and urinary excretion contribute to PhIP clearance in nonanesthetized mice, [^{14}C]PhIP (1 mg/kg) was administered i.v. to *Bcrp1*$^{-/-}$, and wild-type mice housed in metabolic cages and fecal and urinary radioactivity was measured. Most of the radioactivity in urine was excreted during the first 0–4 h. Radioactivity in feces was at its highest between 4 and 8 h and lower in the later time fractions (data not shown). In wild-type mice, 70.4 ± 8.1% of the administered radioactivity was recovered from the feces over the 48 h after administration of [^{14}C]PhIP, indicating that fecal excretion is the main excretory pathway for [^{14}C]PhIP (Fig. 4). Fecal excretion diminished 2.7-fold in *Bcrp1*$^{-/-}$ mice (26.6 ± 5.0%, $P < 0.0001$). This suggests a prominent role for Bcrp1 in the fecal excretion of [^{14}C]PhIP. Radioactivity

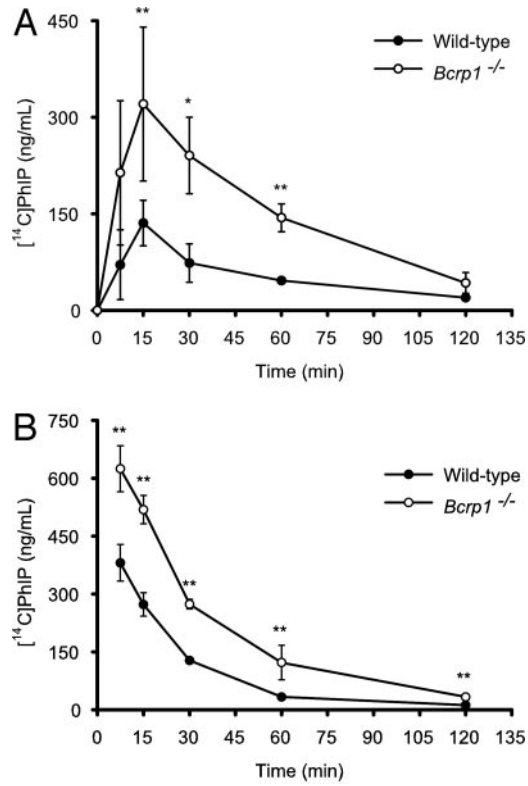

Fig. 3. Plasma concentration *versus* time curve after oral (*A*) and i.v. (*B*) administration of [^{14}C]PhIP (1 mg/kg) to wild-type (●) and *Bcrp1*$^{-/-}$ (○) mice. Data are expressed as average; *error bars* (sometimes smaller than the symbols) indicate SD (n = 3–5; *, $P < 0.05$, **, $P < 0.01$).

excretion had shifted to the urinary route, which was 2.4-fold increased in *Bcrp1*$^{-/-}$ compared with wild-type mice (79.3 ± 15.3 *versus* 33.0 ± 2.5%, $P < 0.0001$; Fig. 4).

Tissue Distribution, Hepatobiliary, and Direct Intestinal Excretion of [^{14}C]PhIP in Gall Bladder-cannulated Mice. To further investigate the role for Bcrp1 in the tissue distribution and excretion of [^{14}C]PhIP, we administered [^{14}C]PhIP (1 mg/kg) i.v. to wild-type and *Bcrp1*$^{-/-}$ mice with a cannulated gall bladder and ligated common bile duct. This set-up allows separate measurement of hepatobiliary and direct intestinal excretion. Radioactivity was measured in several tissues 1 h after i.v. [^{14}C]PhIP administration. Most tissues reflected the 2.4-fold higher plasma [^{14}C]PhIP levels found in *Bcrp1*$^{-/-}$ *versus* wild-type mice (Table 1). There was a relatively high accumulation of radioactivity in the kidney. Radioactivity levels in testis, spleen, and brain were comparatively low (Table 1). The [^{14}C]PhIP levels were considerably higher in small intestinal tissue of wild-type *versus* *Bcrp1*$^{-/-}$ mice, especially when corrected for the lower plasma levels. This higher tissue level probably reflects the much higher accumulation and concentration of [^{14}C]PhIP in the contents of the small intestine of wild-type mice (Table 1): the percentage of the dose [^{14}C]PhIP retrieved from the content of small intestines after 1 h was 2.8-fold higher in wild-type compared with *Bcrp1*$^{-/-}$ mice (4.2 ± 1.5 *versus* 1.5 ± 0.8%, $P < 0.004$; Fig. 5), indicating Bcrp1-mediated transport of [^{14}C]PhIP directly into the lumen of this organ. In the same experiment, we also measured the biliary excretion of [^{14}C]PhIP in fractions of 10 min. All bile fractions from *Bcrp1*$^{-/-}$ animals demonstrated a significantly decreased excretion of [^{14}C]PhIP into bile compared with wild-type mice ($P < 0.0004$; Fig. 6). At 1 h after i.v. administration, the cumulative [^{14}C]PhIP excretion, as percentage of the dose, was 9.0 ± 4.4% *versus* 36.5 ± 9.4% in *Bcrp1*$^{-/-}$ and wild-type mice, respectively. This indicates that 75% of the [^{14}C]PhIP biliary excretion over 1 h can be attributed to Bcrp1 function [1- (0.090/0.365)]. We conclude from these experiments that the hepatobiliary elimination of [^{14}C]PhIP (at this dosage) in mice is extensive and dominated by Bcrp1 activity.

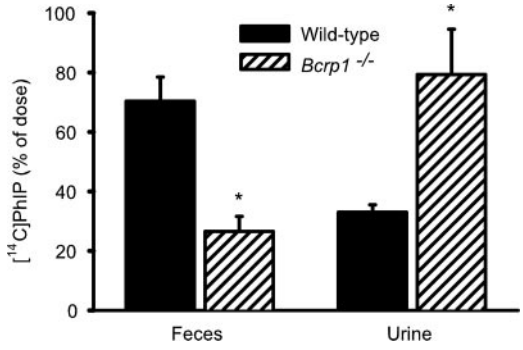

Fig. 4. Fecal and urinary excretion of [^{14}C]PhIP in wild-type and *Bcrp1*$^{-/-}$ mice housed in metabolic cages for 48 h. [^{14}C]PhIP (1 mg/kg) was administered i.v. to *Bcrp1*$^{-/-}$ and wild-type mice that were housed in metabolic cages, and radioactivity was measured in feces and urine excreted between 0–48 h after administration. Data are expressed as percentage of the dose ± SD ($n = 6$; *, $P < 0.0001$ compared with wild type).

Table 1 *Levels of radioactivity in anesthetized gall bladder-cannulated male wild-type and Bcrp1*$^{-/-}$ *mice at 60 min. after i.v. administration of 1 mg/kg [^{14}C]PhIP*

Tissue	Wild-type	*Bcrp1*$^{-/-}$	Ratio $^{-/-}$/wt
Plasma	239.5 ± 91.4	574.0 ± 114.5[a]	2.4
Brain	72.2 ± 18.4	199.0 ± 64.3[a]	2.8
Testis	120.6 ± 19.3	313.0 ± 52.2[a]	2.6
Spleen	454.4 ± 149.3	781.0 ± 349.1	1.7
Kidney	6794.4 ± 1390.0	15578.6 ± 4474.4[a]	2.3
Liver	1294.8 ± 290.8	1928.3 ± 406.3[b]	1.5
Small intestine	2060.9 ± 340.4	1098.4 ± 389.4[a]	0.5
Cecum	1563.9 ± 299.0	1215.0 ± 425.7	0.8
Colon	798.8 ± 147.5	855.5 ± 478.3	1.1
Content small intestine	6801.1 ± 1096.8	2106.1 ± 550.3[a]	0.3
Content cecum	2279.4 ± 597.8	989.4 ± 275.0[a]	0.4
Content colon	2488.7 ± 889.2	1548.4 ± 623.0	0.6

Results are expressed as average [^{14}C]-concentrations (ng-equivalent g^{-1} or ml^{-1}) ± SD (n = 6; [a], $P < 0.01$; [b], $P < 0.05$).

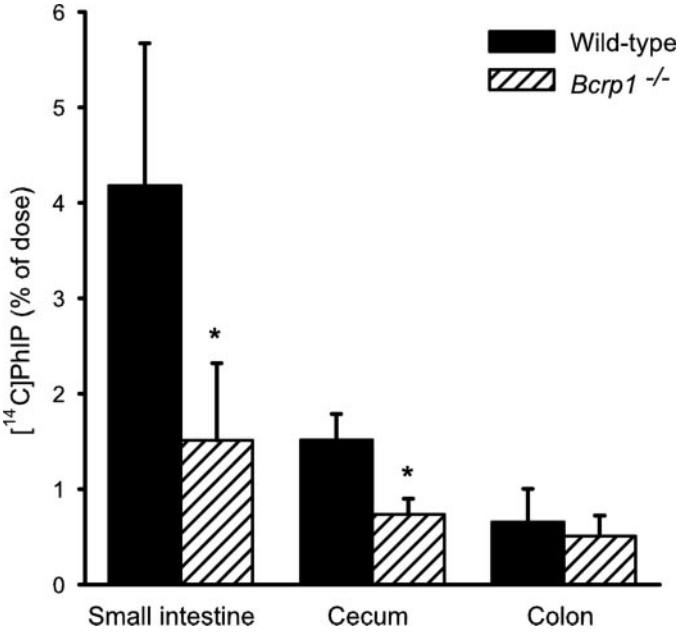

Fig. 5. Intestinal excretion in wild-type and *Bcrp1*$^{-/-}$ mice with a cannulated gall bladder 1 h after i.v. administration of [^{14}C]PhIP (1 mg/kg). Data are expressed as percentage of the dose ± SD ($n = 6$) of radioactivity measured in the contents of small intestine, cecum, and colon (*, $P < 0.004$).

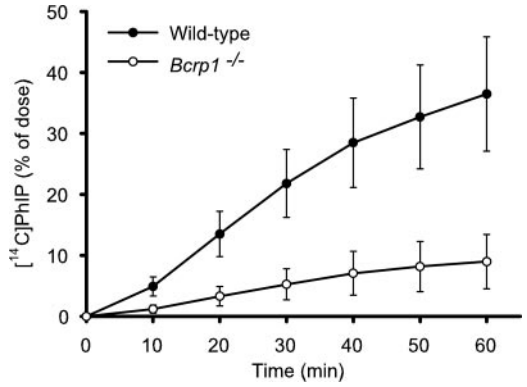

Fig. 6. Cumulative hepatobiliary excretion of [^{14}C]PhIP in wild-type and *Bcrp1*$^{-/-}$ mice. [^{14}C]PhIP was administered i.v. to mice with a cannulated gall bladder. Radioactivity was measured in bile fractions of *Bcrp1*$^{-/-}$ (○) and wild-type (●) mice. Data are expressed as percentage of the dose ± SD ($n = 6$; At all time points $P < 0.0004$).

DISCUSSION

In this study, we demonstrate that the dietary carcinogen PhIP is an efficiently transported substrate of murine Bcrp1. From the Bcrp1-knockout studies, it is clear that this transport results in pronounced effects on the pharmacokinetics of PhIP in mice, leading to substantially decreased bioavailability, increased plasma clearance, and hence markedly altered tissue levels of PhIP. Our analysis also directly demonstrated that murine Bcrp1 is a major factor in the hepatobiliary and direct intestinal excretion of PhIP, resulting in predominantly fecal elimination of PhIP, which was shifted toward predominantly

urinary elimination in mice lacking Bcrp1. Overall, it is clear that Bcrp1 has a profound effect on the exposure of mice to PhIP. As PhIP has been demonstrated to induce colon, prostate, and breast carcinomas in rats and lymphomas in mice, it may well be that Bcrp1 activity will also affect the susceptibility of rodents to PhIP-dependent carcinogenesis.

Extrapolating these results to humans, it is possible that BCRP will affect the susceptibility of humans to PhIP-induced carcinogenesis because human BCRP and mouse Bcrp1 appear to be very similar with respect to transported substrates (23). Inhibition of BCRP by drug intake, as well as the existence of BCRP polymorphisms, can cause inter- and intraindividual variation in BCRP activity (19, 20). Possibly, induction and stimulation of BCRP by food and drug intake is also involved. This may affect the exposure to food carcinogens such as PhIP, with possible consequences for individual differences in cancer susceptibility. Some dose optimization strategies for drugs with narrow therapeutic windows involve the coadministration of transporter inhibitors. When such inhibitors [for instance GF120918 (28)] are applied chronically to increase the oral availability of P-gp and BCRP substrate drugs, they may thereby also increase the bioavailability of PhIP and possibly other food carcinogens. Given these considerations, it will be of interest to address the possible consequences of variation in BCRP/Bcrp1 activity for dietary carcinogen susceptibility, using the *Bcrp1*$^{-/-}$ mouse model as a tool.

We found a comparatively minor role in [^{14}C]PhIP transport for Mdr1a P-gp *in vitro*, and no indication for significant effects of Mdr1a P-gp *in vivo*. In addition, we did not detect significant transport of [^{14}C]PhIP by human MRP2 *in vitro*. This appears to contrast with the study of Dietrich *et al.* (21), who did observe *in vitro* transport of PhIP in the same cell line, albeit at very low concentration (50 nM). Despite the low PhIP transport by human MRP2, *in vivo* studies of PhIP in wild-type and Mrp2-deficient rats revealed pharmacokinetic effects that appear to be quantitatively comparable with what we observed in *Bcrp1*$^{-/-}$ mice with respect to PhIP oral availability and hepatobiliary excretion. In fact, Dietrich *et al.* (22) could attribute a 77% decrease in hepatobiliary excretion of PhIP to loss of Mrp2 activity. Although the PhIP dosage used in the rat studies was probably lower than in our mouse study, it is striking that we found a 75% decrease in hepatobiliary excretion of PhIP because of absence of murine Bcrp1. Taken together, these studies suggest that both Mrp2 and Bcrp1 can play a major role in the hepatobiliary disposition and oral availability of PhIP, although there may also be species differences between rats, mice, and humans in this respect. In any case, in future studies it will be interesting to assess the relative impact of BCRP/Bcrp1 and MRP2/Mrp2 on dietary carcinogens.

Whereas AUCs p.o. between *Bcrp1*$^{-/-}$ and wild-type mice differ 2.9-fold, the oral availability of PhIP (AUC p.o./AUC i.v.) is only modestly increased in *Bcrp1*$^{-/-}$ mice (from 60% in wild-type to 79% in *Bcrp1*$^{-/-}$ mice) because of a 2.2 fold higher AUC i.v. As is also evident from the hepatobiliary and direct intestinal elimination data, this indicates a more pronounced role for Bcrp1 in hepatobiliary elimination of PhIP compared with directly reducing uptake of PhIP from the intestine.

The absence of Bcrp1 resulted in a major shift of PhIP elimination from predominantly fecal to predominantly renal elimination. At first sight, this might seem somewhat surprising because a high level of Bcrp1 is found in the renal proximal tubules (18), and its absence in the *Bcrp1*$^{-/-}$ mice would be expected to result in a decreased renal elimination of PhIP. Apparently, however, when the hepatobiliary and direct intestinal elimination of PhIP is nearly abrogated in *Bcrp1*$^{-/-}$ mice, the kidney can still readily eliminate the excess of PhIP. This might occur primarily by glomerular filtration or perhaps also by other remaining active renal transporters for PhIP (such as Mrp2). The higher plasma PhIP levels in the *Bcrp1*$^{-/-}$ mice will no doubt also enhance this renal elimination.

The tissue distribution of [^{14}C]PhIP was particularly interesting for brain because some studies show that BCRP is present in the human blood-brain barrier in analogy with P-gp (29), and preliminary immunohistochemistry data also suggest Bcrp1 presence in mouse brain capillaries (data not shown). For this single time point, however, at least for PhIP as a substrate, we did not observe a significantly increased brain penetration in Bcrp1$^{-/-}$ mice when corrected for the increased plasma level. Allowing for the limitations of a single time point experiment, the results suggest that Bcrp1 does not play a major role in restricting brain penetration of PhIP.

Finally, we note that this study adds yet another functional class to the growing number of transported BCRP/Bcrp1 substrates. Next to a range of anticancer drugs, dyes such as Hoechst 33342 used for selecting stem cells (30), and pheophorbide a, a natural phototoxin derived from chlorophyll (18), a relatively small HA carcinogen also appears to be part of the substrate spectrum. In view of the considerable diversity in size, structure, and charge (ranging from weak bases to negatively charged compounds such as methotrexate) and biological functions of known BCRP/Bcrp1 substrates, one can reasonably expect that many more medically and toxicologically relevant compounds will also be affected by this transporter.

REFERENCES

1. Zheng, W., Gustafson, D. R., Sinha, R., Cerhan, J. R., Moore, D., Hong, C. P., Anderson, K. E., Kushi, L. H., Sellers, T. A., and Folsom, A. R. Well-done meat intake and the risk of breast cancer. J. Natl. Cancer Inst. (Bethesda), *90:* 1724–1729, 1998.
2. Felton, J. S., Knize, M. G., Shen, N. H., Lewis, P. R., Andresen, B. D., Happe, J., and Hatch, J. T. The isolation and identification of a new mutagen from fried ground beef: 2-amino-1-methyl-6-phenylimidazo[4,5-b]pyridine (PhIP). Carcinogenesis (Lond.), *7:* 1081–1086, 1986.
3. Ito, N., Hasegawa, R., Sano, M., Tamano, S., Esumi, H., Takayama, S., and Sugimura, T. A. new colon and mammary carcinogen in cooked food, 2-amino-1-methyl-6-phenylimidazo[4,5-b]pyridine (PhIP). Carcinogenesis (Lond.), *12:* 1503–1506, 1991.
4. Gross, G. A., Turesky, R. J., Fay, L. B., Stillwell, W. G., Skipper, P. L., and Tannenbaum, S. R. Heterocyclic aromatic amine formation in grilled bacon, beef and fish and in grill scrapings. Carcinogenesis (Lond.), *14:* 2313–2318, 1993.
5. Wakabayashi, K., Ushiyama, H., Takahashi, M., Nukaya, H., Kim, S. B., Hirose, M., Ochiai, M., Sugimura, T., and Nagao, M. Exposure to heterocyclic amines. Environ. Health Perspect., *99:* 129–133, 1993.
6. Ushiyama, H., Wakabayashi, K., Hirose, M., Itoh, H., Sugimura, T., and Nagao, M. Presence of carcinogenic heterocyclic amines in urine of healthy volunteers eating normal diet, but not in patients receiving parenteral alimentation. Carcinogenesis (Lond.), *12:* 1417–1422, 1991.
7. Layton, D. W., Bogen, K. T., Knize, M. G., Hatch, F. T., Johnson, V. M., and Felton, J. S. Cancer risk of heterocyclic amines in cooked foods: an analysis and implications for research. Carcinogenesis (Lond.), *16:* 39–52, 1995.
8. Manabe, S., Tohyama, K., Wada, O., and Aramaki, T. Detection of a carcinogen, 2-amino-1-methyl-6-phenylimidazo[4,5-b]pyridine (PhIP), in cigarette smoke condensate. Carcinogenesis (Lond.), *12:* 1945–1947, 1991.
9. Ishiguro, Y., Ochiai, M., Sugimura, T., Nagao, M., and Nakagama, H. Strain differences of rats in the susceptibility to aberrant crypt foci formation by 2-amino-1-methyl-6-phenylimidazo[4,5-b]pyridine: no implication of Apc and Pla2g2a genetic polymorphisms in differential susceptibility. Carcinogenesis (Lond.), *20:* 1063–1068, 1999.
10. Esumi, H., Ohgaki, H., Kohzen, E., Takayama, S., and Sugimura, T. Induction of lymphoma in CDF1 mice by the food mutagen, 2-amino-1-methyl-6-phenylimidazo[4,5-b]pyridine. Jpn. J. Cancer Res., *80:* 1176–1178, 1989.
11. Shirai, T., Cui, L., Takahashi, S., Futakuchi, M., Asamoto, M., Kato, K., and Ito, N. Carcinogenicity of 2-amino-1-methyl-6-phenylimidazo[4,5-b]pyridine (PhIP) in the rat prostate and induction of invasive carcinomas by subsequent treatment with testosterone propionate. Cancer Lett., *143:* 217–221, 1999.
12. Imaida, K., Hagiwara, A., Yada, H., Masui, T., Hasegawa, R., Hirose, M., Sugimura, T., Ito, N., and Shirai, T. Dose-dependent induction of mammary carcinomas in female Sprague-Dawley rats with 2-amino-1-methyl-6-phenylimidazo[4,5-b]pyridine. Jpn. J. Cancer Res., *87:* 1116–1120, 1996.
13. Hasegawa, R., Sano, M., Tamano, S., Imaida, K., Shirai, T., Nagao, M., Sugimura, T., and Ito, N. Dose-dependence of 2-amino-1-methyl-6-phenylimidazo[4,5-b]pyridine (PhIP) carcinogenicity in rats. Carcinogenesis (Lond.), *14:* 2553–2557, 1993.
14. Sinha, R., Gustafson, D. R., Kulldorff, M., Wen, W., Cerhan, J. R., and Zheng, W. 2-Amino-1-methyl-6-phenylimidazo[4,5-b]pyridine, a carcinogen in high-temperature-cooked meat, and breast cancer risk. J. Natl. Cancer Inst. (Bethesda), *92:* 1352–1354, 2000.

15. Doyle, L. A., Yang, W., Abruzzo, L. V., Krogmann, T., Gao, Y., Rishi, A. K., and Ross, D. D. A multidrug resistance transporter from human MCF-7 breast cancer cells. Proc. Natl. Acad. Sci. USA, *95:* 15665–15670, 1998.
16. Miyake, K., Mickley, L., Litman, T., Zhan, Z., Robey, R., Cristensen, B., Brangi, M., Greenberger, L., Dean, M., Fojo, T., and Bates, S. E. Molecular cloning of cDNAs which are highly overexpressed in mitoxantrone-resistant cells: demonstration of homology to ABC transport genes. Cancer Res., *59:* 8–13, 1999.
17. Jonker, J. W., Smit, J. W., Brinkhuis, R. F., Maliepaard, M., Beijnen, J. H., Schellens, J. H. M., and Schinkel, A. H. Role of breast cancer resistance protein in the bioavailability and fetal penetration of topotecan. J. Natl. Cancer Inst. (Bethesda), *92:* 1651–1656, 2000.
18. Jonker, J. W., Buitelaar, M., Wagenaar, E., van der Valk, M. A., Scheffer, G. L., Scheper, R. J., Plösch, T., Kuipers, F., Oude Elferink, R. P. J., Rosing, H., Beijnen, J. H., and Schinkel, A. H. The breast cancer resistance protein protects against a major chlorophyll-derived dietary phototoxin and protoporphyria. Proc. Natl. Acad. Sci. USA, *99:* 15649–15654, 2002.
19. Imai, Y., Nakane, M., Kage, K., Tsukahara, S., Ishikawa, E., Tsuruo, T., Miki, Y., and Sugimoto, Y. C. 421A polymorphism in the human breast cancer resistance protein gene is associated with low expression of Q141K protein and low-level drug resistance. Mol. Cancer Ther., *1:* 611–616, 2002.
20. Zamber, C. P., Lamba, J. K., Yasuda, K., Farnum, J., Thummel, K., Schuetz, J. D., and Schuetz, E. G. Natural allelic variants of breast cancer resistance protein (BCRP) and their relationship to BCRP expression in human intestine. Pharmacogenetics, *13:* 19–28, 2003.
21. Dietrich, C. G., de Waart, D. R., Ottenhoff, R., Schoots, I. G., and Oude Elferink, R. P. J. Increased bioavailability of the food-derived carcinogen 2-amino-1-methyl-6-phenylimidazo[4,5-b]pyridine in MRP2-deficient rats. Mol. Pharm., *59:* 974–980, 2001.
22. Dietrich, C. G., de Waart, D. R., Ottenhoff, R., Bootsma, A. H., van Gennip, A. H., and Oude Elferink, R. P. J. Mrp2-deficiency in the rat impairs biliary and intestinal excretion and influences metabolism and disposition of the food-derived carcinogen 2-amino-1-methyl-6-phenylimidazo[4,5-b]pyridine (PhIP). Carcinogenesis (Lond.), *22:* 805–811, 2001.
23. Allen, J. D., van Loevezijn, A., Lakhai, J. M., van der Valk, M., van Tellingen, O., Reid, G., Schellens, J. H. M., Koomen, G. J., and Schinkel, A. H. Potent and specific inhibition of the breast cancer resistance protein multidrug transporter *in vitro* and in mouse intestine by a novel analogue of fumitremorgin C. Mol. Cancer Ther., *1:* 417–425, 2002.
24. Schinkel, A. H., Wagenaar, E., van Deemter, L., Mol, C. A. A. M., and Borst, P. Absence of the mdr1a P-glycoprotein in mice affects tissue distribution and pharmacokinetics of dexamethasone, digoxin and cyclosporin A. J. Clin. Investig., *96:* 1698–1705, 1995.
25. Smit, J. W., Weert, B., Schinkel, A. H., and Meijer, D. K. F. Heterologous expression of various P-glycoproteins in polarized epithelial cells induces directional transport of small (type 1) and bulky (type 2) cationic drugs. J. Pharmacol. Exp. Ther., *286:* 321–327, 1998.
26. Evers, R., Kool, M., van Deemter, L., Janssen, H., Calafat, J., Oomen, L. C. J. M., Paulusma, C. C., Oude Elferink, R. P. J., Baas, F., Schinkel, A. H., and Borst, P. Drug export activity of the human canalicular multispecific organic anion transporter in polarized kidney MDCK cells expressing cMOAT (MRP2) cDNA. J. Clin. Investig., *101:* 1310–1319, 1998.
27. De Bruin, M., Miyake, K., Litman, T., Robey, R., and Bates, S. E. Reversal of resistance by GF120918 in cell lines expressing the ABC half-transporter, MXR. Cancer Lett., *146:* 117–126, 1999.
28. Kruijtzer, C. M., Beijnen, J. H., Rosing, H., ten Bokkel Huinink, W. W., Schot, M., Jewell, R. C., Paul, E. M., and Schellens, J. H. M. Increased oral bioavailability of topotecan in combination with the breast cancer resistance protein and P-glycoprotein inhibitor GF120918. J. Clin. Oncol., *20:* 2943–2950, 2002.
29. Cooray, H. C., Blackmore, C. G., Maskell, L., and Barrand, M. A. Localisation of breast cancer resistance protein in microvessel endothelium of human brain. Neuroreport, *13:* 2059–2063, 2002.
30. Zhou, S., Morris, J. J., Barnes, Y., Lan, L., Schuetz, J. D., and Sorrentino, B. P. Bcrp1 gene expression is required for normal numbers of side population stem cells in mice, and confers relative protection to mitoxantrone in hematopoietic cells *in vivo.* Proc. Natl. Acad. Sci. USA, *99:* 12339–12344, 2002.